

Determination of Volume Fraction of a Glass Fibre/ Matrix Composite Plate using Vibration Analysis

N. I. E. Farhana^{1*}, M. S. Abdul Majid¹, M. P. Paulraj¹ and E. Ahmadhildi²

¹School of Mechatronic Engineering, University Malaysia Perlis, Arau, Malaysia; farhanaizwani@gmail.com, shukry@unimap.edu.my, paul@unimap.edu.my

²Advanced Material Research Centre (AMREC), SIRIM Berhad, Kulim, Malaysia; hildi@sirim.my

Abstract

Currently, the volume fraction of a glass fibre/matrix based composite material is being assessed only by destructive techniques. Instead of changing or destroying the structure, a new non-destructive approach based on vibration technique is proposed in this research. Further, the main objective of this paper is on the determination of fibre/matrix volume fractions using vibration analysis. A complete experimental protocol has been developed to record the vibration signals produced from experimental plates with different volume fractions and thicknesses. The recorded vibration signals were analyzed both in time and frequency domains. Subsequently, statistical parameter features from each thickness was extracted and associated to the volume fraction levels. Artificial Neural Network (ANN) models were then developed to classify the level of volume fraction. The classification performance of the developed network models were in the range of 80-98 percent. From the results, it has been observed that the network model with frequency band based features has yielded a better classification performance. This proves that the method implemented can be used as the alternatives to the ASTM D2584-11 for determination of volume fraction of a glass fibre/matrix composite plate using vibration analysis.

Keywords: Composite, Feed-Forward Neural Network, Non-Destructive Testing, Statistical Features, Vibration Signal, Volume Fraction

1. Introduction

Normally all composite materials will react well with the surroundings. Many researches have analyzed the performances of different composite materials in order to prove their advantages over conventional materials. It has been reported that materials with lower volume fraction are widely used for fabricating different types of structures¹. The mechanical properties of composites are derived from the properties such as deformation of layer structure between fiber and resin, the mixture and the fibre volume fraction². The mechanical properties of a material are influential in designing the composite structure³. Therefore, many researchers focused on the

study related to the mechanical properties and to contribute more towards the composite field. The strength and the mechanical behavior of materials depend upon the bonding between fibre and matrix and this will directly leads to the impact performance of the materials. Various investigations over the effect of Glass Fiber Reinforced Polymer (GFRP) composition on the impact behavior were studied with contradictory results⁴. The method currently employed for determining the volume fraction of composite materials are through acid digestion, optical microscopy-based method and ignition loss method. The primary disadvantage of destructive testing is that an actual section of the composite material must be destroyed in order to determine the volume fraction. This will defi-

*Author for correspondence

nitely waste the materials by changing or destroying their usefulness. Further, this method is not environmentally friendly as it involves a burning process, acidic solution and many more. In order to safely determine the volume fraction, a simple non-destructive approach is proposed in this research work. The main focus in this paper is to develop the fundamental understanding on how the non-destructive method can be used to determine the volume fraction of the composite materials and to show that even by using a simple laboratory test, the volume fraction of glass fibre can be determined. Non-Destructive Testing (NDT) is a clean analysis technique which is widely used in industry or even in science field to investigate the properties of a material, system or component without involving any damage. In other words, after the test or experiment is done, the tested part can still be used⁵. NDT used in this research work is the based on analyzing the vibration pattern produced in different composite materials. Hence, in this work we present experimental results containing to the vibration pattern of glass fibre/matrix plate composite under free vibration condition. Vibration analysis on the effect of fibre matrix composition on the impact performance of GFRP was extensively studied by numerous researchers that lead to different results⁶⁻¹⁰. However, free vibration analysis of laminated composite plates and shells based on artificial intelligent has not received ample attention.

In this study, a simple experimental arrangement is developed based on a simply supporting boundary condition to record the distribution of vibration signals of glass fibre composite plates with different volume fraction. Data capturing protocol is proposed to record the vibration motion by subjecting the experimental plate to an external impact excitation. The vibration signals recorded at various node points are then analyzed both in time and frequency domain. The results obtained are compared. Frequency bands are analyzed and the statistical features are extracted as features. The extracted features are then validated through Analysis of Variance (ANOVA). The validated extracted features are then associated to the respective plate's composite volume fraction. Subsequently, a network model is trained with Levenberg Marquardt (LM) method.

This paper is separated into three subsections; protocol, feature extraction and artificial neural networks for classification.

2. Protocol

Using LMS SCADAS Mobile as Data Acquisition system (DAQ), the vibration at various node points is recorded. The LMS system has a signal analyzer which can be used to perform time and frequency domain analysis. LMS system was used to model test based on hammering method. Hence, the corresponding frequency response can be obtained and analyzed. The LMS SCADAS Mobile workstation along with the impact hammer and accelerometer sensor is shown in Figure 1.

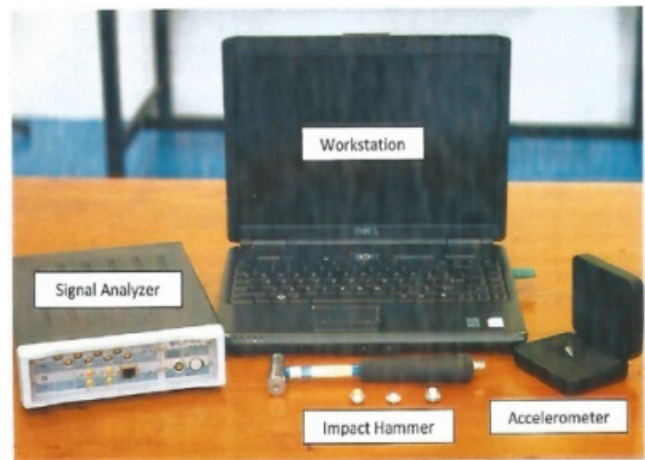


Figure 1. LMS SCADAS mobile workstation.

2.1 Sensors and Force Transducer

In most of the vibration monitoring application, accelerometers are the most preferred motion sensors. They can be used to measure signals of low to very high frequencies and are available in a variety of general purpose and application-specific designs. The piezoelectric accelerometer is reliable, versatile, unmatched for frequency and amplitude range and popular for machinery monitoring. The piezoelectric accelerometer (model: 3055B1T) with an input sensitivity of 10 mV/g ($g=9.82 \text{ m/s}^2$) is used in this experimental work. The impact hammer used in this research work is from Dytran 5800B2-50LbF range, 100 mV/LbF).

2.2 Pre-Experimental Setup

Numerous conventional manufacturing techniques used to fabricate the composite material; wet layup, pre-preg layup, compression moulding, resin infusion, filament

winding and etc. In this work, 12 laminated glass fibre composite plates with different volume fractions and thicknesses were manufactured using a compression moulding machine as shown in Figure 2. This technique is normally used in industries since it holds good for small production runs and also it gives out a very good compressed plates as compared to other techniques. The mass of the 12 composite plates are tabulated in Table 1.

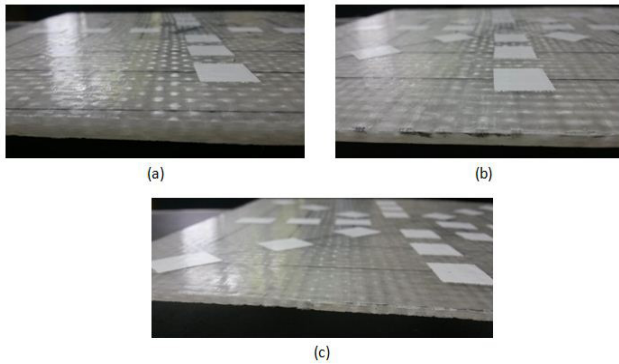


Figure 2. Experimental plates with thickness: (a) 5 mm; (b) 3 mm; (c) 2 mm.

Table 1. List of thickness, volume fraction and mass of glass-fibre composite plates

| Thickness (mm) | Volume Fraction (%) | Mass (g) |
|----------------|---------------------|----------|
| 5.5 | 35.0 | 590 |
| 5.7 | 40.0 | 660 |
| 5.5 | 45.0 | 631 |
| 5.8 | 50.0 | 746 |
| 3.0 | 31.5 | 326 |
| 3.0 | 38.2 | 370 |
| 3.0 | 42.0 | 374 |
| 3.0 | 57.6 | 307 |
| 2.0 | 28.3 | 219 |
| 2.0 | 37.0 | 237 |
| 2.2 | 48.2 | 270 |
| 2.8 | 26.7 | 285 |

The experimental samples are then cut into dimensions of 25.4 x 25.4 mm² respectively. The classification process was conducted by considering 5 mm, 3 mm and 2 mm in thickness.

The fabricated composite plates are then segmented so as to form three concentric squares. The innermost concentric square cell is labelled as I₁, I₂, I₃, I₄, middle and outer are labelled as m₁, m₂, m₃, m₄ and o₁, o₂, o₃, o₄ respectively. The three concentric square cells are segmented so as to make I₁m₁ = m₁o₁ = I₂m₂ = m₂o₂ = I₃m₃ = m₃o₃ = I₄m₄ = m₄o₄. The centre of the concentric cell is marked as C. The segmented concentric square along with the node points are shown in Figure 3a and Figure 3b shows the experimental plate with cell division.

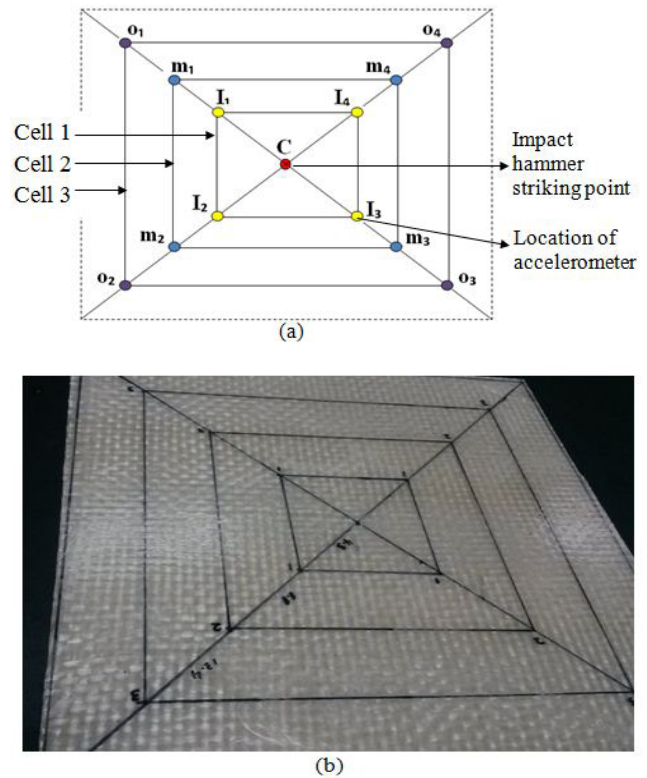


Figure 3. Pre-experimental setup protocol: (a) plate alignment lay out; (b) the experimental plate with cell division.

A simple supporting structure is intended to support the experimental plates in free-free boundary condition. According to the literature survey, various researchers^{5,11} used different types of supporting structure for free boundary condition such as elastically supporting the entire surface, plate suspended using a string and supported with sponge at the corners of a plate or along the



Figure 4. Glass-fibre plate pivoted by cushioned nails.

edges. A small modification to the above test setup may lead to a totally different result; appropriate actions are to be offered to design a more accurate test setup. After considering the advantages and disadvantages of the various experimental setup models, some improvements made in designing the framework that is by using sponges supported by a nail with diameter 2 mm glued to the plate and the entire arrangement was placed on a rubber mattress. Many researchers used the sponges in the experimental setup as it involves in recording the vibration signal. The sponges have further minimized the effect of plate bounce and supposed the noise saved in the recorded vibration

sounds. The glued nails helped to reduce the contact area between the plate and the supporting structure shown in Figure 4. The diameter of the nail sharp point should be as minimal as possible.

2.3 Data Acquisition System

The first input channel of the LMS system is connected to the impact hammer. Three accelerometers are then connected to the remaining three input channel. The impact hammer is used to generate an impulse force by striking the hammer at the centre point of the plate. This impact then produces vibrations throughout the

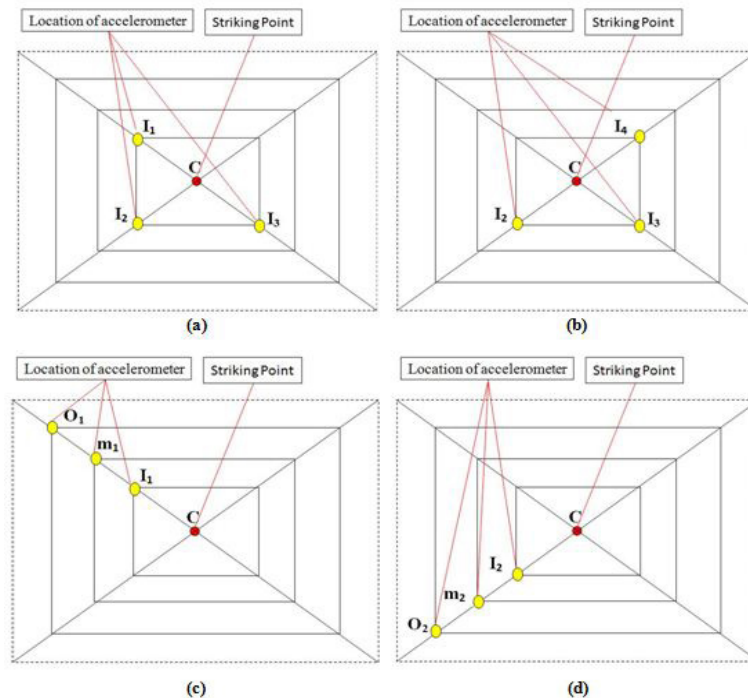


Figure 5. Typical nodal measurement position: (a) $I_1 I_2 I_3$; (b) $I_2 I_3 I_4$; (c) $I_1 m_1 o_1$; (d) $I_2 m_2 o_2$.

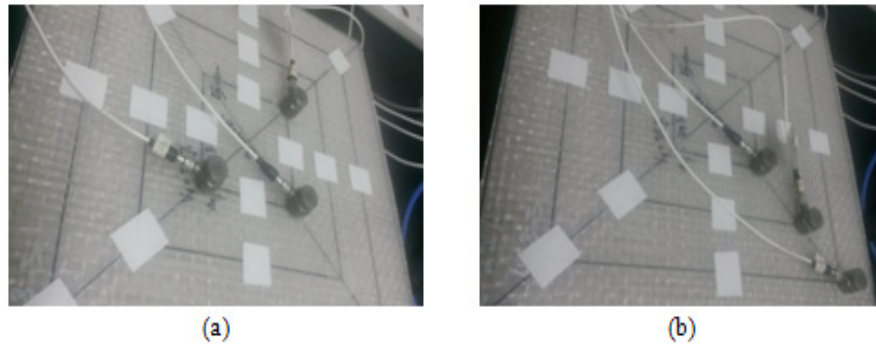


Figure 6. Typical nodal measurement position on experimental plate: (a) $I_1I_2I_3$; (b) $I_1m_1o_1$.

plate's surface. The vibration level at various node points are then recorded by placing accelerometers at the node points. Initially, the impact affect in the inner square is studied by placing the accelerometers at the node points I_1, I_2 and I_3 . An impulse pulse is produced by striking the impact hammer at point C and the vibration signals were measures at I_1, I_2 and I_3 . Five such trials were formed. A similar procedure was followed and the vibration signals at the corners of the inner square namely, $I_1I_2I_3, I_2I_3I_4, I_3I_4I_1$ and $I_4I_1I_2$ produced due to the impulse signal at C were recorded. Further, the above procedure is also repeated for the middle and outer squares and the vibration effect at $m_1m_2m_3, m_2m_3m_4, m_3m_4m_1, m_4m_1m_2, o_1o_2o_3, o_2o_3o_4, o_3o_4o_1$ and $o_4o_1o_2$ were recorded. Similarly, the vibration signal due to the impact at C was also measured at $I_1m_1o_1, I_2m_2o_2, I_3m_3o_3$ and $I_4m_4o_4$ by placing the accelerometer at the appropriate node points. Typical model measurement positions are shown in Figure 5 and Figure 6.

The impulse force and vibration level at the various node points are recorded for 10 seconds at a sampling frequency 1024 Hz. All the recorded signals were saved in default DAQ file format '.xdf', which were then exported as Microsoft '.wav' file format for further analysis through MATLAB.

2.4 Data Preprocessing

The recorded vibration signal contains change in energy level information for a period of 10 seconds. Since the recording period is fixed (10 second) and the time instant of hammer strike is a variable parameter, the time at which the peak value occurred in the recorded signal is considered as the reference point for further analysis. From the recorded signal, the time at which the peak value occur (t_p) is first determined and then the signals recorded from

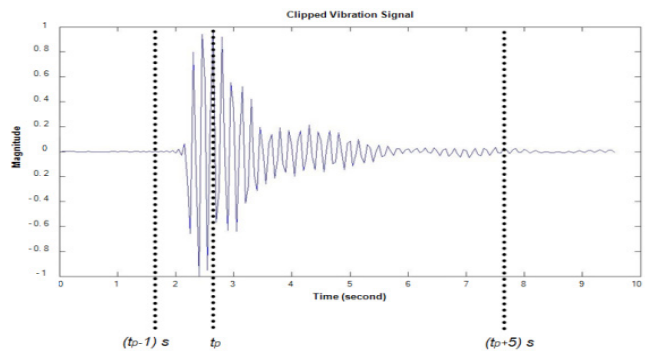


Figure 7. Typical clipped vibration signal.

($t_p - 1$ sec) to ($t_p + 5$ sec) are extracted and used in the further feature extraction process. A typical signal extraction in the above process is shown in Figure 7. By considering the signal from 1 s to 5 s, the final length of the clipped signal is 6144 Hz at a sampling frequency of 1024 Hz samples per second.

2.5 Feature Extraction

2.5.1 Time Domain Statistical Features Extraction

All time domain-features do not require complex pre-processing, for example, it does not require the laborious task of filtering, Fourier transformation, framing, windowing and much more complex analysis. Time domain only takes a small power to process; however, it directly deploys the algorithms only at the constrained nodes¹². Consequently, in this work the features are extracted using time domain approach based statistical features. The definition of all the extracted time features is presented in this section.

2.5.1.1 Mean (μ)

The mean μ is defined as the average value of the vibration signal. The mean value of the signal can be computed by using Equation 1.

$$\mu = \frac{1}{N} \sum_{i=1}^N x_i \quad (1)$$

2.5.1.2 Standard Deviation (σ)

It is similar to the average deviation, except the averaging is done with power instead of amplitude of the signal and is computed using Equation 2.

$$\sigma = \frac{1}{N} \sum_{i=1}^N (x_i - x_\mu)^2 \quad (2)$$

2.5.1.3 Variance (σ^2)

The variance is the square root of the standard deviation from the signal and can be computed using Equation 3.

$$\sigma^2 = \frac{1}{N} \sum_{i=1}^N (x_i - x_\mu)^2 \quad (3)$$

2.5.1.4 Simple Square Integral (S_i)

Integral square can be defining as the total energy of the signal and can be computed using Equation 4.

$$S_i = \frac{1}{N} \sum_{i=1}^N (|x_i|)^2 \quad (4)$$

2.5.1.5 Root Mean Square (Erms)

The root mean square is a statistical measure features that represent the input power of the vibration signal and is calculated using Equation 5.

$$E_{rms} = \sqrt{\frac{1}{N} \sum_{i=1}^N x_i^2} \quad (5)$$

2.5.1.6 Kurtosis (k)

Kurtosis (k) is the distribution level of peakedness, define

as a normalized form of the fourth central moment of a distribution and can be computed using Equation 6.

$$k = \frac{1}{N} \sum_{i=1}^N \left(\frac{x_i - x_\mu}{x_\sigma} \right)^4 \quad (6)$$

2.5.1.7 Mean Power (μ_p)

Mean power can be defined as the total energy level throughout the vibration signal and can be calculated using Equation 7.

$$\mu_p = \frac{x_\mu}{N} \sum_{i=1}^N (x_i)^2 \quad (7)$$

2.5.1.8 Skewness (sw)

Skewness is the distribution level of asymmetry or to be more exact, the lack of symmetry. The signal is symmetric if it has a stable ratio from left to right of the middle point and can be computed using Equation 8.

$$sw = \frac{1}{N} \sum_{i=1}^N \left(\frac{x_i - x_\mu}{x_\sigma} \right)^3 \quad (8)$$

2.5.1.9 Average Absolute Value (AA)

Average Absolute value is defined as the mean magnitude of the signal and can be calculated using Equation 9.

$$AA = \frac{1}{N} \sum_{i=1}^N |x_i| \quad (9)$$

Where: x_i = i^{th} of the vibration signal
 N = total number of elements in the signal
 x_μ = mean value of the signal
 x_σ = the standard deviation of the signal.

2.5.2 Frequency Domain Feature Extraction

All frequency domain features require preprocessing and Fast Fourier Transformation (FFT). Therefore, in this work, two approaches are proposed for frequency domain analysis that is by extracting the frequency information

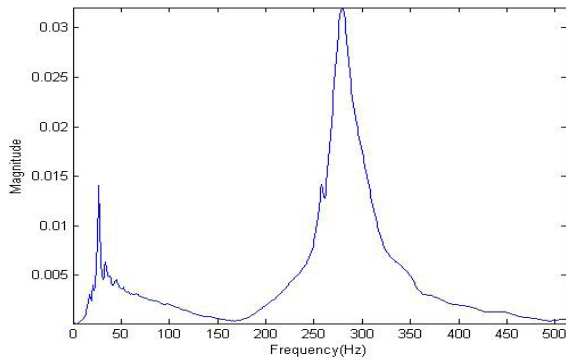


Figure 8. Typical magnitude plot of the FFT.

from FFT and by dividing the FFT into numbers of band. Both the results are then compared.

2.5.3 Computing the FFT

From time domain signal, the frequency information is extracted by computing the Discrete Fourier Transform (DFT) based Fourier transform algorithm to reduce the computation time. The Fourier Transform produces a complex number output signal which can be displayed with two signals, either with real and imaginary part or with magnitude and frequency. In signal processing, mostly the magnitude of the Fourier Transform is framed-up, as it contains most of the information from the time domain signal. Figure 8 shows the sample graph of the magnitude extracted after performing Fourier Transform.

Further, the statistical based features are then extracted from the whole FFT signal. The extracted frequency domain features can be represented as:

2.5.3.1 Entropy (S)

Entropy can be defined as average measure of data contained in the signal and can be calculated using Equation 10.

$$S = -\sum_{f=1}^{N_f} x_f \log x_f \tag{10}$$

2.5.3.2 Mean Frequency (μ_f)

The mean is defined as the average value of the Fourier Transform signal and can be calculated using Equation 11.

$$\mu_f = \frac{1}{N_f} \sum_{f=1}^{N_f} x_f \tag{11}$$

2.5.3.3 Mean Power (μ_{pf})

Power can be defined as the total energy level throughout the Fourier Transform signal and can be calculated using Equation 12.

$$\mu_{pf} = x_{\mu f} \sum_{f=1}^{N_f} (x_f)^2 \tag{12}$$

2.5.3.4 Standard Deviation (σ_f)

The σ_f is similar with average deviation, except the average is done with power instead of amplitude of the Fourier Transform and is computed using Equation 13.

$$\sigma_f = \frac{1}{N_f} \sum_{f=1}^{N_f} (x_f - x_{\mu f}) \tag{13}$$

2.5.3.5 Variance (σ_f^2)

The variance is the square root of the standard deviation from the Fourier Transform signal and can be computed using Equation 14.

$$\sigma_f^2 = \frac{1}{N_f} \sum_{f=1}^{N_f} (x_f - x_{\mu f})^2 \tag{14}$$

2.5.3.6 Total Power (tp)

Total power can be define as the total amount of the energy stored in the Fourier Transform signal. The total power can be calculated using Equation 15.

$$t_p = \sum_{f=1}^{N_f} x_f \tag{15}$$

2.5.3.7 Median Frequency (Md)

Median frequency is define as a frequency value at which the vibration signal power spectrum is divided into two regions with an equal integrated power¹³ and can be calculated using Equation 16.

$$Md = \frac{1}{2} \sum_{f=1}^{N_f} t_p \tag{16}$$

2.5.3.8 Peak Frequency (Pf)

Peak Frequency or sometimes known as dominant frequency is the maximum energy in the power spectrum and can be compute using Equation 17.

$$Pf = \sum_{f=1}^{N_f} \max x_f \tag{17}$$

2.5.3.9 Power Spectrum Ratio (PSR)

PSR is a ratio between the maximum energy in vibration signal power spectrum and the whole energy of vibration signal power spectrum¹⁶. It can be calculated using Equation 18.

$$PSR = \sum_{f=1}^{N_f} \frac{Pf}{t_p} \tag{18}$$

2.5.3.10 Spectral Moment (SM)

Spectral Moment (SM1-SM3) known as the content at every frequency in the spectrum is weighted by the kth power of the frequency and the result is summed up

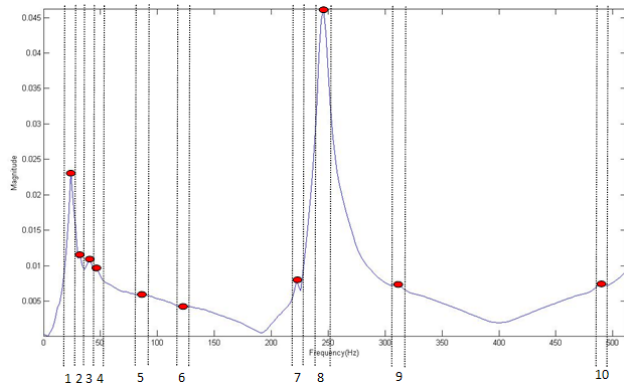


Figure 9. Typical plot of extracted frequency band from FFT.

Table 2. Frequency band

| Band No | Frequency Range |
|---------|-----------------|
| Band 1 | 23Hz-27Hz |
| Band 2 | 31Hz-35Hz |
| Band 3 | 38Hz-42Hz |
| Band 4 | 45Hz-49Hz |
| Band 5 | 85Hz-89Hz |
| Band 6 | 121Hz-125Hz |
| Band 7 | 220Hz-224Hz |
| Band 8 | 244Hz-248Hz |
| Band 9 | 307Hz-311Hz |
| Band 10 | 488Hz-492Hz |

across the entire spectrum. It can be calculated using Equation 19.

$$SM = \sum_{f=-\infty}^{f=\infty} f^k x_f \tag{19}$$

Where: N_f = the length of frequency.
 $x_{\mu f}$ = mean value of the vibration signal power spectrum.
 $x_f = f^h$ of the vibration signal power spectrum.

2.5.4 Frequency Bands Feature Extraction

After performing the Fourier Transform the frequency range is divided into frequency band. The frequency peak (fp) is identified and divided into number of bands. The frequency band is considered by choosing the lower band frequency at 2 Hz before the peak occurred and the upper band frequency at 2 Hz after the occurrence of the peak value. The selected frequency bands are shown in Figure 9.

The set of features are extracted from these respective frequency bands. The selected ten different bands along with their band frequency range are shown in Table 2.

Further, the statistical based features that have been applied in the analysis of individual frequency band of vibration signal are peak frequency, median frequency and power spectrum ratio. The definition for all these variables is presented as in the previous section.

As a summary for feature extraction method, nine time domain statistical features are extracted that form 27

Table 3. Features validation for three vibration channel

| Thickness | Features Extracted | | | | | |
|-----------|--------------------|-------|------------------|-------|----------------|-------|
| | Time Domain | | Frequency Domain | | Frequency Band | |
| | Before | After | Before | After | Before | After |
| 2 mm | 27 | 23 | 36 | 36 | 90 | 64 |
| 3 mm | 27 | 26 | 36 | 27 | 90 | 71 |
| 5 mm | 27 | 21 | 36 | 36 | 90 | 80 |

Table 4. Removed extracted features for frequency band

| Band | Removed Extracted Features for 3 Channel (CH) | | | | | | | | | |
|------|---|-----------------|----------|-----------------|-----------|-----------|------|----------|------|-----|
| | Thickness | | | | | | | | | |
| | 2 mm | | | 3 mm | | | 5 mm | | | |
| | CH 1 | CH 2 | CH 3 | CH 1 | CH 2 | CH 3 | CH 1 | CH 2 | CH 3 | |
| 1 | PSR | PSR Md Pf | Md Pf | PSR Md Pf | PSR | PSR | PSR | | - | |
| 2 | - | | Md Pf | Md Pf | | | PSR | - | - | PSR |
| 3 | - | | PSR | | | | | PSR | Md | - |
| 4 | - | PSR | | PSR | Md PSR | Md PSR | - | - | - | |
| 5 | PSR | PSR | - | PSR | - | - | - | PSR | - | |
| 6 | - | - | - | - | - | - | PSR | - | - | |
| 7 | - | - | - | - | - | - | - | Md Pf | - | |
| 8 | - | - | - | - | - | - | PSR | | - | |
| 9 | - | - | - | - | - | - | - | - | PSR | |
| 10 | Md Pf | Md Pf | Md Pf | - | - | - | - | - | - | |

Table 5. Removed extracted features for time and frequency domain

| Thickness | Domain | Removed Features for 3 Channels | | |
|-----------|-----------|---------------------------------|----------------------|-----------|
| | | CH 1 | CH 2 | CH 3 |
| 2 mm | Time | - | μ, sw | μ, sw |
| | Frequency | - | - | - |
| 3 mm | Time | μ | - | - |
| | Frequency | μ_{pf}, tp, Md | | |
| 5 mm | Time | μ, μ_{pf} | μ, S_p, μ_{pf} | μ |
| | Frequency | - | - | - |

final features vectors since the features are extracted from three accelerometers. Similarly for frequency domain based Fourier Transform signal, 12 extracted features that form 36 features vectors and 3 features are extracted from 10 individual frequency bands then forming 90 features vectors respectively. All the extracted features from time and frequency domain database are formulated for further analysis.

3. Feature Validation

A primary issue in modeling the feature is the feature validation process, which concerns the meaning of a feature, given by its information content. The extracted features are then validated using Analysis of Variance (ANOVA) by taking the mean value for each feature. The result for the number of features before validation and after validation is as shown in Table 3.

As can be seen in Table 3, the number of features reduced after performing the data validation. The results shown in Table 4 summarised the removed frequency band features as each band validating different features. The extracted features that were removed from the three channels for time and frequency domain are tabulated in Table 5.

The validation conducted helps the system to better understand the classification process. The information from training and testing database were defined based on the validated extracted features.

Volume fractions were then associated with the validated extracted features. Thus a database consists of

extracted features from time and frequency domain associated to the volume fractions has been formulated.

4. Artificial Neural Network

4.1 Artificial Neural Network (ANN)

An Artificial Neural Network is a data transforming framework that has been created to mimic the numerical model for human cognition. ANN is a modelling tool based on nonlinear statistical data that model the complicated network within input and output in order to find a pattern. Network contains three layers specifically; hidden, input and output layer. Basically, neural networks are constructed in layers that made up in various interconnected 'nodes' that have 'activation function' in it. The 'input layer' represent the pattern to the network that impart with one or more 'hidden layers'. This is where the real processing is taking part through weighted 'connections' system. The output layer will link with hidden layer to determine the output of the network which is the answer.

There are several types of ANN; feed-forward neural network, kohonen self-organizing network, Radial Basis Function (RBF), physical neural network and etc. Based on the extracted feature vectors, feed-forward neural system is developed, modeled and trained. The feed-forward neural network is the first and the simplest type of ANN devised. The neural network training parameters are sets by default in MATLAB software but hidden neuron and

Table 6. Classification accuracy for thickness 2 mm

| Trial | Output Neuron: 4 | | | | Total samples: 320 | |
|-------------|------------------|--------|------------------|-------|--------------------|-------|
| | Time Domain | | Frequency Domain | | Frequency Band | |
| | IN: 23 | HN: 12 | IN: 36 | HN:18 | IN:64 | HN:35 |
| 1 | 83.4 | | 97.5 | | 97.5 | |
| 2 | 85.0 | | 93.4 | | 95.3 | |
| 3 | 87.8 | | 96.6 | | 98.4 | |
| 4 | 85.9 | | 95.9 | | 97.2 | |
| 5 | 79.1 | | 97.5 | | 96.6 | |
| 6 | 90.9 | | 95.9 | | 97.2 | |
| 7 | 90.0 | | 96.3 | | 96.6 | |
| 8 | 85.9 | | 96.3 | | 97.2 | |
| 9 | 82.5 | | 95.3 | | 94.7 | |
| 10 | 81.9 | | 98.4 | | 97.2 | |
| Mean | 85.24 | | 96.31 | | 96.79 | |

*IN=Input Neuron; HN=Hidden Neuron

Table 7. Classification accuracy for thickness 3 mm

| Trial | Output Neuron: 4 | | | | Total samples: 320 | |
|-------------|------------------|--------|------------------|-------|--------------------|-------|
| | Time Domain | | Frequency Domain | | Frequency Band | |
| | IN: 26 | HN: 13 | IN: 27 | HN:14 | IN:71 | HN:36 |
| 1 | 81.3 | | 86.6 | | 97.8 | |
| 2 | 81.9 | | 89.4 | | 97.8 | |
| 3 | 72.9 | | 86.6 | | 99.1 | |
| 4 | 74.4 | | 85.3 | | 99.1 | |
| 5 | 85.0 | | 87.8 | | 97.8 | |
| 6 | 79.7 | | 88.8 | | 98.4 | |
| 7 | 88.8 | | 95.9 | | 96.3 | |
| 8 | 87.5 | | 83.8 | | 98.1 | |
| 9 | 82.5 | | 90.3 | | 98.8 | |
| 10 | 75.0 | | 88.1 | | 97.2 | |
| Mean | 80.90 | | 88.26 | | 98.04 | |

*IN=Input Neuron; HN=Hidden Neuron

Table 8. Classification accuracy for thickness 5 mm

| Trial | Output Neuron: 4 | | | | Total samples: 320 | |
|-------------|------------------|--------|------------------|-------|--------------------|-------|
| | Time Domain | | Frequency Domain | | Frequency Band | |
| | IN: 21 | HN: 11 | IN: 36 | HN:18 | IN:80 | HN:40 |
| 1 | 91.9 | | 76.9 | | 97.8 | |
| 2 | 93.8 | | 80.3 | | 96.6 | |
| 3 | 93.1 | | 81.6 | | 97.5 | |
| 4 | 89.1 | | 80.9 | | 95.3 | |
| 5 | 90.3 | | 84.7 | | 95.3 | |
| 6 | 78.4 | | 80.9 | | 97.8 | |
| 7 | 93.1 | | 80.9 | | 95.0 | |
| 8 | 79.4 | | 80.3 | | 97.5 | |
| 9 | 77.5 | | 81.9 | | 95.9 | |
| 10 | 83.4 | | 82.8 | | 94.4 | |
| Mean | 87.0 | | 81.12 | | 96.31 | |

*IN=Input Neuron; HN=Hidden Neuron

output neurons are optimally chosen based on the features while training the network.

The dataset is randomly divided into two datasets namely, training set and testing set. The training set used to train the system; in the meantime the testing set is to validate the network model. The training set used in this work is 70 percent from the samples.

4.2 Feed Forward Neural Networks

A simple feed-forward neural network is modeled and trained using Levenberg Marquardt algorithm. The modelled network consists of an input layer with number of input neurons being equal to the number of input features in the dataset. The 'trainlm' function available in MATLAB neural network was used to model the neural network. The neural networks were trained using 70 percent (224 samples) of the database and tested with remaining 30 percent testing data samples.

5. Results

All the trained neural network models were validated with the testing samples. The details about the network architecture member namely the number of input neuron, hidden neuron and output neurons along with classification performance of the network models are shown in Tables 6, 7 and 8.

From Tables 6, 7 and 8, it can be observed that the network model developed using the frequency band based statistical features has yielded the highest classification performance for all the thickness as compared to the time and frequency domain based network models. The network model developed using frequency band based statistical features has the highest classification for all the thickness while the network model developed using frequency domain features has the lowest classification accuracy of 81.12% for 5 mm thickness respectively.

6. Conclusion

This paper presents the experimental procedure to record and analyse the vibration signal propagated through composite plate. Statistical based time and frequency domain features were extracted. The features were then validated through ANOVA. The validated extracted features were then associated to the glass fibre's volume fraction to form final features matrix. A simple feed-forward neural network were developed and trained to classify the volume fractions. The training results show that frequency band features can be used to classify the volume fraction of composite materials with good agreement.

7. Acknowledgement

The authors would like to acknowledge the support and encouragement by Universiti Malaysia Perlis and Majlis Amanah Rakyat (MARA) for the financial support. This study was conducted at University Malaysia Perlis.

8. References

1. Khalid AA. The effect of testing temperature and volume fraction on impact energy of composites. *Mater Des.* 2006 Jan; 27(6):499–506.
2. El Messiry M. Theoretical analysis of natural fiber volume fraction of reinforced composites. *Alexandria Eng J.* 2013 Sep; 52(3):301–6.
3. Abdalla F, Megat M, Sapuan M, Sahari BB. Determination of volume fraction values of filament wound glass and carbon fiber reinforced composites. *ARPJ Eng Appl Sci.* 2008; 3(4):7–11.
4. Badawy AAM. Impact behavior of glass fibers reinforced composite laminates at different temperatures. *Ain Shams Eng J.* 2012 Jun; 3(2):105–11.
5. Ioan C. Contents aspects concerning to the free vibration of the rectangular plate made of glass / rubber composite. 15th International Research/Expert Conference on Trends in the Development of Machinery and Associated Technology. 2011 Sep. p. 625–8.
6. Inventic E. The modal analysis of plates. *Analysis.* 2011; 8204(1):2–5.
7. El-Soaly E, Sultan R, Younes SGM. Delamination detection of composite laminates using natural frequency. *Int hour-nal Mech Eng Robot Res.* 2012 Jul; 1(2):286–96.
8. Kant T, Kommineni JR. Large amplitude free vibration analysis of cross-ply composite and sandwich laminates with a refined theory and finite elements. *Comput Struct.* 1994 Mar; 50(1):123–34.
9. Reddy MRS. Prediction of natural frequency of laminated composite plates using Artificial Neural Networks. *Engineering.* 2012 Jun; 04(6):329–37.
10. Paulraj MP, Yaacob S, Abdul Majid MS, Kazim MNFM, Krishnan P. Structural steel plate damage detection using non destructive testing, frame energy based statistical features and artificial neural networks. *Procedia Eng.* 2013; 53:376–86.
11. Hatami S, Azhari M, Saadatpour MM. Free vibration of moving laminated composite plates. *Compos Struct.* 2007 Oct; 80(4):609–20.
12. Thongpanja S, Phinyomark A, Phukpattaranont P, Limsakul C. Mean and median frequency of EMG signal to determine muscle force based on time dependent power spectrum. *Elektron. ir Elektrotehnika.* 2013; 19(3):51–6.
13. Dargie W. Analysis of time and frequency domain features of accelerometer measurements. *Proceedings of International Conference Computer Communication Networks (ICCCN);* 2009 Aug. p. 1-6.